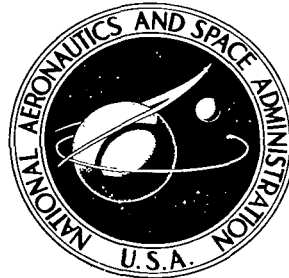


NASA TECHNICAL NOTE



NASA TN D-5095

e.1

LOAN COPY: RETURN TO
AFWL (WLIL-2)
KIRTLAND AFB, N ME

0131792



NASA TN D-5095

**NONCAVITATING AND CAVITATING
PERFORMANCE OF SEVERAL LOW AREA
RATIO WATER JET PUMPS HAVING
THROAT LENGTHS OF 3.54 DIAMETERS**

by Nelson L. Sanger

*Lewis Research Center
Cleveland, Ohio*



NONCAVITATING AND CAVITATING PERFORMANCE OF SEVERAL
LOW AREA RATIO WATER JET PUMPS HAVING THROAT
LENGTHS OF 3.54 DIAMETERS

By Nelson L. Sanger

Lewis Research Center
Cleveland, Ohio

NATIONAL AERONAUTICS AND SPACE ADMINISTRATION

For sale by the Clearinghouse for Federal Scientific and Technical Information
Springfield, Virginia 22151 - CFSTI price \$3.00

ABSTRACT

Performance of several jet pumps was determined for pumps having diffuser included angles of 2.5° and 6° over a range of spacings of the nozzle exit from the throat entrance of 0 to 3.0 throat diameters. The throat length was found to be too short to permit matching with a conventional diffuser (6° included angle) because significant mixing continued into the diffuser entrance. However, due to the low rate of diffusion the pump having the 2.5° diffuser achieved the relatively high efficiencies of 31.5 percent for a nozzle-to-throat area ratio of 0.066, and 38.7 percent for an area ratio of 0.197.

CONTENTS

	Page
SUMMARY	1
INTRODUCTION	2
PERFORMANCE ANALYSIS	3
Principle of Operation	3
Analyses	4
Assumptions	4
Basic parameters	4
Noncavitation analysis	4
Cavitation analysis	5
APPARATUS AND PROCEDURE	5
Test Pump	5
Apparatus	8
Test facility	8
Instrumentation	8
Experimental Procedure	9
RESULTS AND DISCUSSION	11
Noncavitation Performance	11
Efficiency and head rise	11
Best efficiency nozzle position	11
Comparison of theory with experiments	13
Effect of flow ratio	15
Effect of nozzle spacing and diffuser angle	15
Effect of throat length	19
Cavitation Performance	22
SUMMARY OF RESULTS	24
APPENDIXES	
A - SYMBOLS	27
B - DETERMINATION OF FRICTION LOSS COEFFICIENTS	29
REFERENCES	31

NONCAVITATING AND CAVITATING PERFORMANCE OF SEVERAL LOW AREA RATIO WATER JET PUMPS HAVING THROAT LENGTHS OF 3.54 DIAMETERS

by Nelson L. Sanger
Lewis Research Center

SUMMARY

The noncavitating and cavitating performance of several jet pumps having throat lengths of 3.54 diameters and diffuser included angles of 2.5° and 6° were evaluated in a water facility for four nozzle-to-throat area ratios ranging between 0.066 and 0.197. Area ratio was varied by using different nozzles. Spacing of the nozzle exit from the throat entrance was varied from 0 to 3.0 throat diameters. Deaerated, room-temperature tap water was used as test fluid.

Objectives of the investigation were: to experimentally determine overall non-cavitating and cavitating performance; to study the mixing characteristics over a wide range of geometrical and flow conditions; to compare the experimental results with those obtained for previously investigated configurations having longer throat lengths; and to compare the overall experimental performance to noncavitating and cavitating theoretically predicted performance.

The highest efficiencies were achieved in the pump having the 2.5° diffuser included angle; 31.5 percent was achieved for an area ratio of 0.066 and 38.7 percent for an area ratio of 0.197. The throat length of 3.54 throat diameters was found to be too short to allow matching with conventional diffusers (approximately 6° included angle) because mixing was incomplete at the diffuser entrance. However, when the short throat was matched with the 2.5° diffuser jet pump efficiency was not penalized because the low rate of diffusion permitted mixing to continue efficiently in the upstream portion of the diffuser; but the small diffuser outlet area of the 2.5° diffuser did not permit high static pressures to be recovered.

The noncavitating analysis did not predict jet pump efficiency and head ratio within an acceptable range of accuracy. This was probably due to the mixing which continued into the diffuser. However, the cavitation analysis, which does not depend on mixing characteristics, predicted the conditions at head-rise deterioration within about 10 percent for the various geometric conditions investigated.

INTRODUCTION

One means of supplying large quantities of continuous, on-board electric power for space vehicles is the use of a Rankine cycle system using liquid metal as the working fluid (refs. 1 and 2). In such systems the condensate return pump must continuously pump fluid at near saturation conditions to the high pressure environment of the boiler. To suppress cavitation in the main condensate return pump the jet pump has been selected (ref. 2) as one possible auxiliary boost pump. Its cavitation resistance, simplicity, and reliability make it well-suited for long-term space applications.

The combination of high boiler pressure and low condenser pressure leads to the selection of jet pumps having low ratios of nozzle exit area-to-throat area (area ratio R). The lack of detailed information on jet pumps in this geometrical category provided the impetus for a program of research on the noncavitating and cavitating performance of low area ratio jet pumps.

In reference 3 a jet pump having a relatively long throat (7.25 diam.) was investigated for two area ratios, $R = 0.066$ and 0.197 . Nozzle spacing was the principal geometric variable investigated, and particular attention was paid to the mixing characteristics in the pump. Measured values of efficiency and head ratio correlated closely with values predicted by a one-dimensional analysis. In reference 4 cavitation performance was examined in detail for the same pumps reported in reference 3. A theoretically-derived cavitation parameter provided good correlation between predicted and measured flow conditions at the point of head-rise deterioration for both area ratios, and over a wide range of nozzle positions.

In reference 5 a shorter throat length (5.66 diam.) pump was investigated for the same two area ratios ($R = 0.066$ and 0.197). The same good correlation of noncavitating and cavitating results with the respective analyses was observed. Furthermore, the reduction in throat length resulted in an improvement in maximum efficiency values at practically every nozzle position.

Because of the need for minimization of weight and size in space electric power-plants, jet pumps of short length are of interest. In the present investigation, jet pumps having throat lengths of 3.54 throat diameters were evaluated. Two test sections were utilized, differing only in diffuser configurations (included angles of 2.5° and 6°). Experimental results from each test section were compared directly to determine the effect of diffuser angle. Results were also compared directly with data from references 3 to 5 to evaluate the effect of throat length. The analysis for noncavitating flow developed in reference 3 and the cavitation prediction parameter developed in reference 4 were applied to the configurations and flow conditions investigated as a further test of their applicability.

Both test sections evaluated were constructed with a circular bellmouth entry and a constant diameter throat having a length of 3.54 diameters. In both cases, the diffusers

were the same length but differed in diffuser included angle (2.5° against 6.0°). Four nozzles, corresponding to area ratios of 0.066, 0.108, 0.141, and 0.197, were used in the test section having a 2.5° diffuser included angle. Two nozzles, corresponding to area ratios of 0.066 and 0.197, were used in the other test section with the 6° diffuser. Spacing of the nozzle exit from the throat entrance was varied between 0 and 3.04 throat diameters. Room-temperature, deaerated tap water was used as test fluid. Primary flow rates varied from 28 to 83 gallons per minute (1.77×10^{-3} to 5.24×10^{-3} m³/sec) and secondary flow rates from 32 to 185 gallons per minute (2.02×10^{-3} to 11.68×10^{-3} m³/sec).

PERFORMANCE ANALYSIS

Principle of Operation

A schematic representation of a jet pump is shown in figure 1 and the symbols and nomenclature are presented in appendix A. The principle of operation of a jet pump is the transfer of energy and momentum from the high velocity primary fluid to the pumped, or secondary fluid, through a process of turbulent mixing.

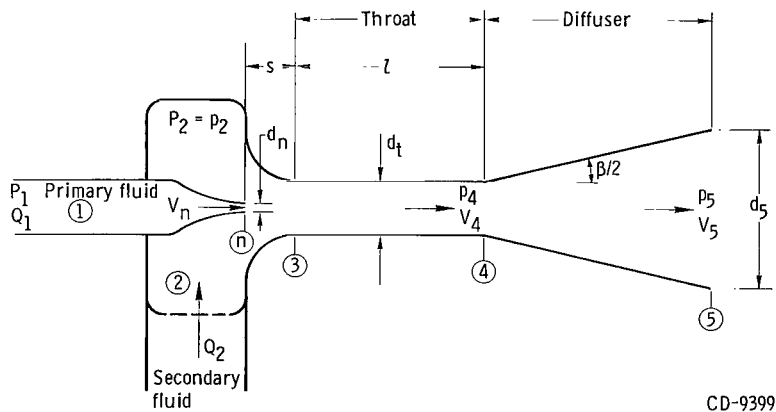


Figure 1. - Schematic representation of jet pump.

The primary fluid is pressurized by an independent source and is accelerated to high velocity in the nozzle. The secondary fluid is entrained by and mixed with the primary fluid in the throat or mixing section. The mixed fluids then pass through the diffuser in which a portion of the kinetic energy (velocity head) is converted to potential energy (static pressure).

The primary fluid leaves the nozzle as a core of high velocity fluid. It is separated from the secondary stream by a thin region of high shear. Turbulent mixing between the

two fluids occurs in the mixing or shear region which grows in thickness with increasing axial distance. The lowest local pressures occur in the shear region (ref. 6) and therefore cavitation inception also takes place in this region.

Analyses

One-dimensional analyses of the noncavitating and cavitating analyses flows are presented in references 3 and 4. Confined-jet mixing analyses (refs. 7 and 8) are not sufficiently developed so that an easily applied jet pump design procedure can be derived. Thus the one-dimensional analyses are generally used; but they must be supplemented by empirical information to determine optimum throat lengths, nozzle positions, diffuser geometry and area ratios for specific applications.

Assumptions. - The assumptions that are common to both the noncavitating and cavitating analyses are:

- (1) Both the primary and secondary fluids are incompressible.
- (2) The temperature of the primary and secondary fluids are equal.
- (3) Nozzle spacing from the throat entrance is zero.
- (4) Nozzle wall thickness is zero.
- (5) An additional assumption is used in the noncavitating analysis; namely, that mixing is complete at the throat exit.

Basic parameters. - There are four fundamental jet pump parameters, all expressed in dimensionless form. These parameters are:

- (1) Nozzle to throat area ratio, $R = A_n/A_t$
- (2) Secondary to primary flow ratio, $M = Q_2/Q_1$
- (3) Head ratio, $N = (H_5 - H_2)/(H_1 - H_5)$
- (4) Efficiency, $\eta = MN$ the equivalent of net output power divided by net input power

A parameter that is useful in the study and comparison of axial static pressure variation in constant diameter jet pumps is the pressure coefficient C_p defined by

$$C_p = \frac{p_x - p_2}{\gamma \frac{V_n^2}{2g}}$$

Noncavitation analysis. - The noncavitation analysis is presented in detail in appendix B of reference 3 (Conventional Analysis). It consists of a one-dimensional application of the continuity, momentum, and energy relations across the individual components of the pump. Friction losses are taken into account with friction loss coefficients K

which are based upon total pressure losses in individual components of the pump, such as the primary nozzle, throat, and diffuser.

The formula for head ratio N resulting from the analysis is

$$N = \frac{2R + \frac{2R^2M^2}{1-R} - R^2(1+M)^2(1+K_t+K_d) - \frac{R^2M^2}{(1-R)^2}(1+K_s)}{1+K_p - 2R - \frac{2R^2M^2}{1-R} + R^2(1+M)^2(1+K_t+K_d)} \quad (1)$$

Determination of the various loss coefficient values is discussed in appendix B.

Cavitation analysis. - The cavitation analysis (appendix B, ref. 4) applies to the conditions at the cavitation-induced total-head breakdown point, rather than to inception conditions.

The analysis consists of an application of the continuity and energy relations to the secondary fluid. Combined with this is the assumption that at the point where the total head falls off the static pressure in the plane of the primary nozzle exit (and throat entrance) is equivalent to the vapor pressure of the fluid. The resulting nondimensional expression for the cavitation prediction parameter is

$$\omega = \frac{P_2 - p_v}{\gamma \frac{V_n^2}{2g}} = \left(\frac{V_3}{V_n} \right)^2 (1 + K_s) \quad (\text{at total head-rise dropoff}) \quad (2)$$

APPARATUS AND PROCEDURE

Test Pump

The test pump (fig. 2) consisted of the following elements: the primary nozzle, the secondary plenum, nozzle spacing shims, and the test section.

The stainless steel plenum upstream of the test section was $15\frac{1}{2}$ inches (39.35 cm) in diameter, and had a capacity of about $4\frac{1}{2}$ gallons ($1.70 \times 10^{-2} \text{ m}^3$). Secondary fluid was supplied to it through two diametrically opposed 3-inch (7.61-cm) outside diameter pipes.

In reference 3 a test section throat of length 7.25 diameters was used primarily as a means of studying the mixing characteristics in the throat. A shorter throat length (5.66 throat diameters) was investigated in reference 5 and resulted in improved performance. If mixing could be efficiently completed in a shorter throat length, lighter and

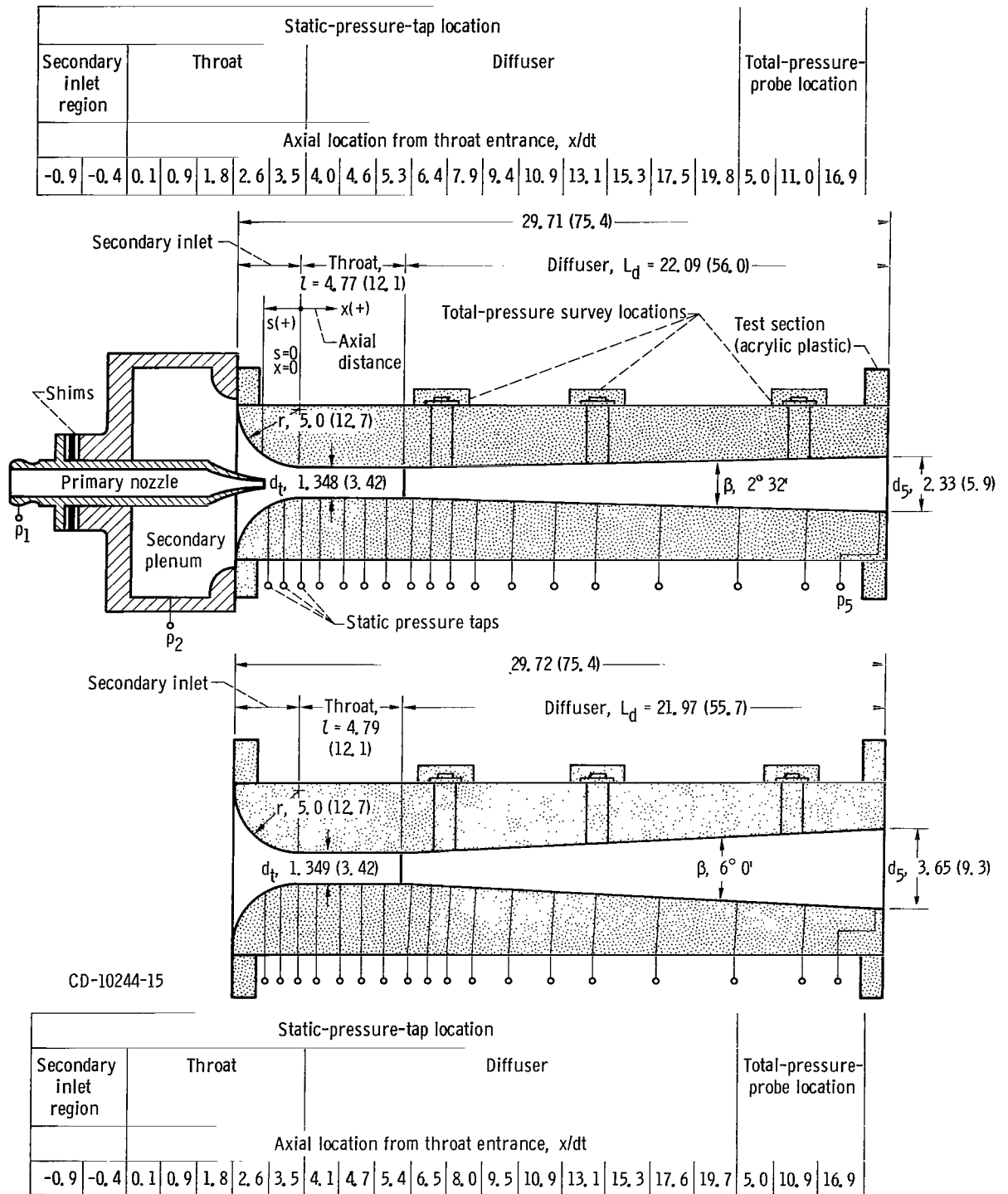


Figure 2 - Schematic diagram of test pumps and location of static-pressure taps and total-pressure probes. (All dimensions are in inches (cm).)

more compact pumps would result. Therefore, the pumps evaluated in the present investigation utilized throat lengths of 3.54 throat diameters. Throat diameter (1.349 in., 3.42 cm) was the same as in references 3 to 5. The test sections were fabricated from transparent acrylic plastic. A 5-inch (12.7-cm) radius bellmouth was used as inlet to the constant diameter throat. The two test sections differed only in diffuser geometry. One had a 2.5° diffuser included angle, the other a 6° included angle. Overall length of both test sections was identical (29.7 in., 75.4 cm). This resulted in a diffuser outlet-to-inlet area ratio of 2.97 for the 2.5° diffuser and 7.32 for the 6° diffuser.

Total pressure probes were mounted in the diffuser at axial locations of 5.0, 11.0, and 16.9 throat diameters, measured from the throat entrance (see fig. 2).

Static pressure taps of 0.020 inch (0.051 cm) in diameter were installed at 18 axial locations (see fig. 2).

The significant dimensions of the four stainless steel primary nozzles used are given in figure 3. The nozzles corresponding to area ratios of 0.066 and 0.197 are the same as those studied in references 3 to 5. The spacing of the nozzle exit from the throat entrance was controlled by the use of shims inserted between the nozzle flange and a reference surface on the plenum.

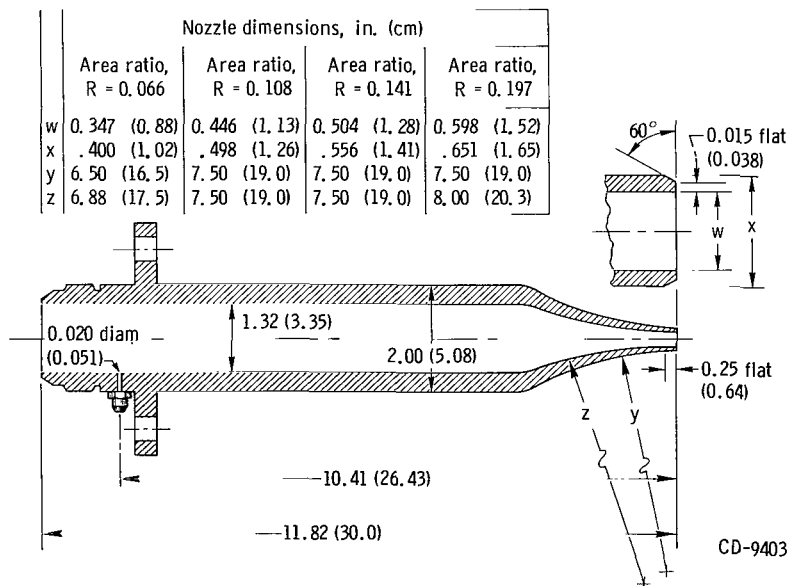


Figure 3. - Jet pump primary nozzles. (All dimensions are in inches (cm).)

Apparatus

Test facility. - The test facility is completely described in reference 3. A schematic diagram of the facility is shown in figure 4. The test facility was a closed loop, continuous circulation water tunnel having a total liquid capacity of about 350 gallons (1.325 m³). Working fluid was deaerated 80° F (300 K) tap water, continuously filtered to remove particles larger than 25 micrometers.

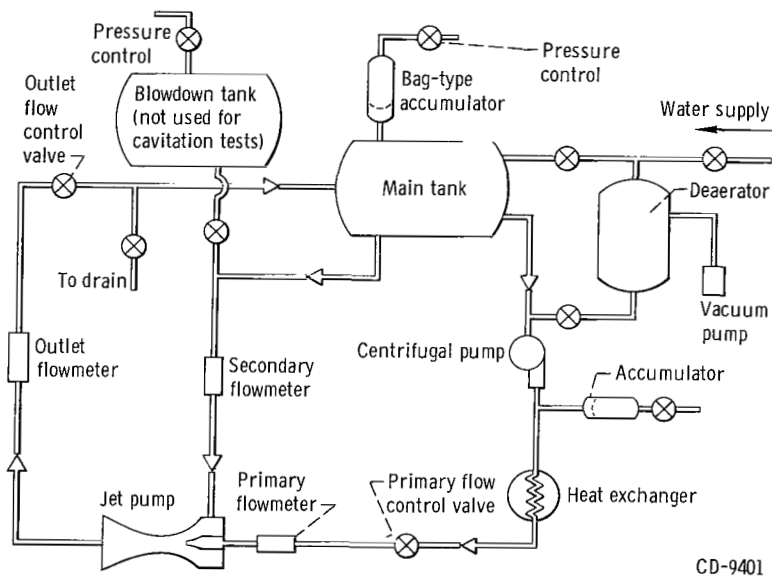


Figure 4. - Schematic drawing of water jet pump test facility.

Instrumentation. - The instrumentation used in this investigation is identical to that used in references 3 to 5. Primary fluid inlet pressure was measured on a Bourdon tube gage. All other pressures presented herein were measured on mercury manometers. Primary and secondary flow rates were measured by turbine flowmeters. Total flow rate was measured by a venturi flowmeter. The venturi-measured flow rate agreed within 2 percent to the sum of the primary and secondary flow rates.

Temperatures were measured in the primary, secondary, and mixed streams by means of copper-constantan thermocouples. Air content was measured with a Van Slyke gas apparatus.

The maximum estimated error of the principal measured variables is listed as follows:

Head rise and static pressure, percent	<±0.7
Inlet pressure (primary stream), percent	<±0.6
Flow rate; primary stream, percent	<±1.0
Flow rate; secondary stream, percent	<±2.0
Temperature, °F (°C)	<±2 (1.1)
Total pressure surveys:	
Total pressure, percent	<±2.0
Radial position, percent	<±5.0

Experimental Procedure

Performance was obtained over a wide range of operating conditions for each nozzle-to-throat area ratio. The ranges of operation for both the noncavitating and cavitating tests are presented in table I.

Noncavitating test runs were conducted at constant values of secondary inlet pressure and primary flow rate. Secondary flow rate, and therefore, flow ratio was varied. This procedure was followed at several nozzle positions for each area ratio. Total pressure surveys were also conducted at selected nozzle positions for each area ratio.

Cavitation performance was obtained at constant values of flow ratio. With both flow rates (and therefore, flow ratio) held constant as secondary inlet pressure P_2 is reduced, head ratio remains constant at the noncavitating value until severe cavitation causes it to deteriorate.

Several values of flow ratio which spanned the noncavitating best efficiency point were selected. Primary flow rate was held constant. At each flow ratio, secondary inlet pressure was reduced in discrete steps from a value corresponding to noncavitating operation, until cavitation caused a sharp drop in total head rise.

Space electric power systems will use liquid metals which have a very low gas content. In order to simulate these conditions the water in the jet pump test facility was deaerated to air contents of 3 parts per million by mass or less.

The flow conditions at total headrise breakdown are of major interest for cavitating operation. Therefore, determination of incipient cavitating conditions are not considered in this report.

TABLE I. - PUMP OPERATING CONDITIONS

Area ratio, R	Nozzle spacing, s/d _t	Primary flow rate, Q ₁		Flow ratio, M	Secondary inlet pressure, P ₂	
		gal/min	m ³ /sec		psia	N/m ²
Noncavitating operation						
0.066	0 to 3.03	28	1.77×10 ⁻³	0.92 to 5.39	15	103×10 ³
		35	2.21	.92 to 5.39		
0.108	0 to 3.03	35	2.21×10 ⁻³	0.66 to 3.84	15	103×10 ³
		50	3.16	.66 to 3.84		
0.141	0 to 3.03	45	2.84×10 ⁻³	0.54 to 3.20	15	103×10 ³
		60	3.79			
0.197	0 to 3.03	63	3.98×10 ⁻³	0.48 to 2.70	15	103×10 ³
		83	5.24	.48 to 2.70		
Cavitating operation						
0.066	0	33	2.08×10 ⁻³	2.0 to 4.5	4.2 to 20.6	29 to 142×10 ³
	1.27					
	2.57					
0.108	0	35	2.21×10 ⁻³	2.60 to 3.60	4.6 to 19.5	32 to 134×10 ³
	.99					
	2.48					
	0	45	2.84×10 ⁻³			
	.99					
	2.48					
0.141	0	45	2.84×10 ⁻³	1.90 to 2.84	4.4 to 21.2	30 to 146×10 ³
	.77					
	2.26					
	0	57	3.60×10 ⁻³			
.77						
2.26						
0.197	0	75	4.74×10 ⁻³	0.90 to 2.15	4.2 to 21.1	29 to 145×10 ³
	1.36					
	1.99					
	2.68					

RESULTS AND DISCUSSION

Noncavitation Performance

Efficiency and head rise. - Jet pump efficiency and head rise are plotted in figures 5(a) and (b), respectively, as functions of flow ratio (M) for the test section having a 2.5° diffuser included angle and an area ratio of $R = 0.197$. Efficiency is plotted for five nozzle positions. As can be observed the peak efficiency and best efficiency flow

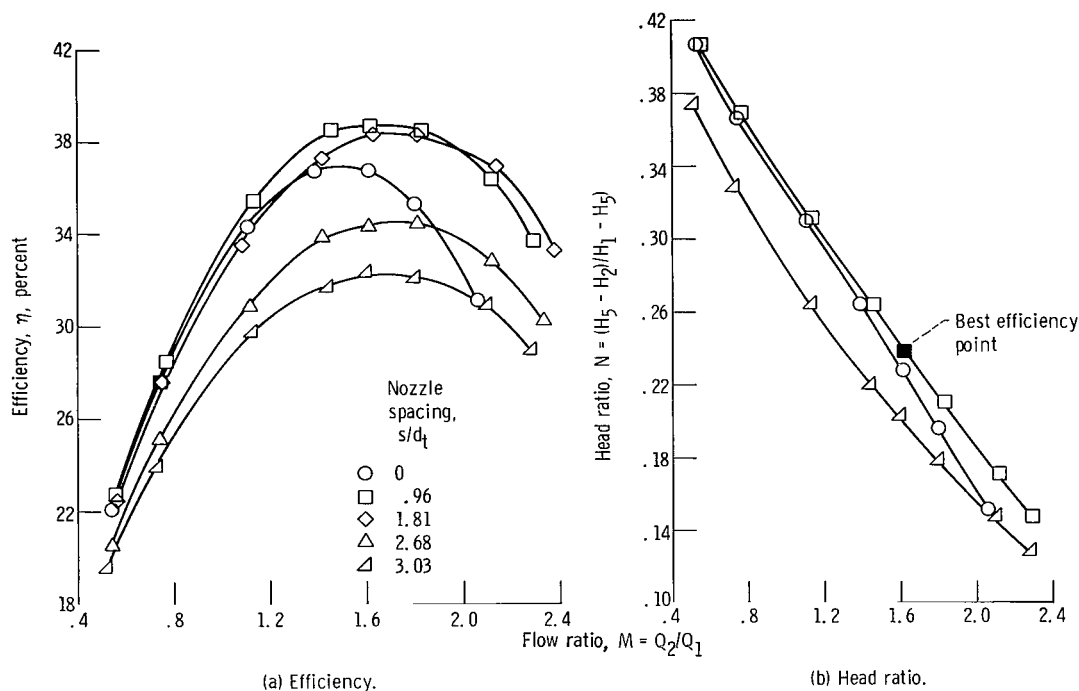


Figure 5. - Noncavitating performance of jet pumps. Area ratio, 0.197; primary flow rate, 63 gallons per minute ($3.97 \times 10^{-3} \text{ m}^3/\text{sec}$); throat length, l/d_t , 3.54; diffuser included angle, 2.5° .

ratio shifted as nozzle spacing was varied. The maximum efficiency, 38.7 percent, achieved at a nozzle spacing of $s/d_t = 0.96$ and a flow ratio of $M = 1.62$, was the highest efficiency measured in the overall experimental program (refs. 3, 5, and this report).

Head ratio is presented in figure 5(b) for three nozzle positions, the fully inserted ($s/d_t = 0$), the best efficiency, and a position in the low efficiency range. Similar curves were obtained for the other configurations and area ratios evaluated.

Best efficiency nozzle position. - Maximum efficiency is presented in figure 6 as a function of nozzle position for the two pumps which differed only in diffuser angle. Performance for two area ratios is presented. It is evident that the pump having the 2.5°

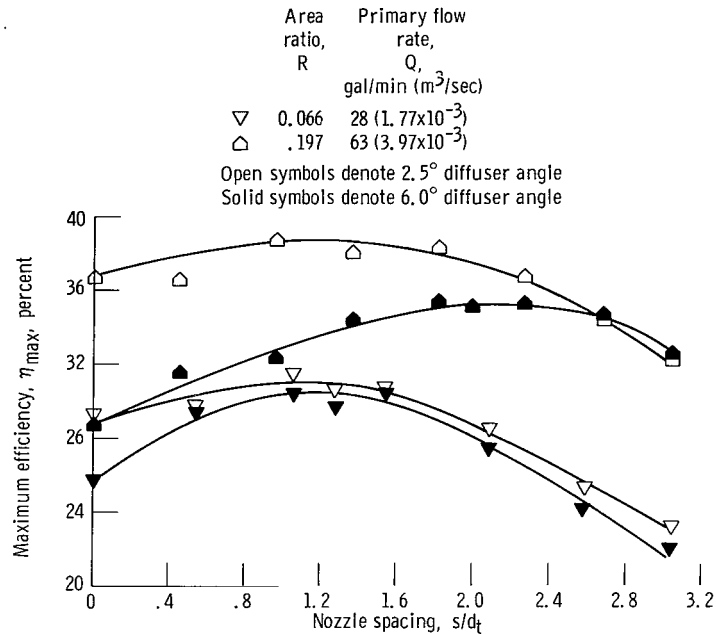


Figure 6. - Effect of diffuser angle on most efficient nozzle position.
Throat length, 3.54.

diffuser angle produced a higher efficiency than the 6^o diffuser angle pump at practically every nozzle position. This is probably due largely to a nonuniform velocity profile at the diffuser inlet of both pumps caused by insufficient throat length to complete mixing. For two diffusers having equal lengths but different included angles, a nonuniform velocity profile has a greater adverse effect on the performance of the wider angle diffuser because of the greater axial static pressure gradient. In a mixing profile the slow moving fluid is near the wall and is analogous to a very thick boundary layer. The adverse pressure gradient in the diffuser acts to further decelerate the slow moving fluid near the wall, resulting in energy losses. As the diffuser angle is increased these losses also increase because the static pressure gradient becomes greater. In reference 9 static pressure recovery of the diffuser was found to be a function of inlet boundary layer conditions. Reductions in recovery resulted as the inlet boundary layer was thickened. Since both diffusers are of the same length, it might be expected that the 6^o diffuser angle pump would perform less efficiently than the 2.5^o pump. Required mixing length to produce acceptable diffuser inlet velocity profiles will be discussed at greater length in the section Effect of nozzle spacing and diffuser angle.

A second effect evident from figure 6 is that at $R = 0.197$ high maximum efficiencies were generally achieved and maintained at greater nozzle spacings than for $R = 0.066$. It was previously noted (refs. 3 and 5) that more mixing length appeared necessary for pumps having area ratios of $R = 0.197$ than for $R = 0.066$. This also

appears to be the case with the present pumps, the additional mixing length being provided by a greater nozzle spacing.

The maximum values of efficiency measured at each nozzle position are also plotted in figure 7 for the four area ratios evaluated with the test section having the 2.5° diffuser included angle. For this jet pump a nominal value for best efficiency nozzle spacing of $s/d_t = 1.0$ appears near optimum. There were improvements in maximum efficiency for all nozzle spacings as area ratio increased, except none was evident in the range $s/d_t = 0$ to 1.0 for an increase of area ratio from 0.141 to 0.197. This lack of improvement at low nozzle spacings is probably also due to greater mixing length requirements as area ratio is increased.

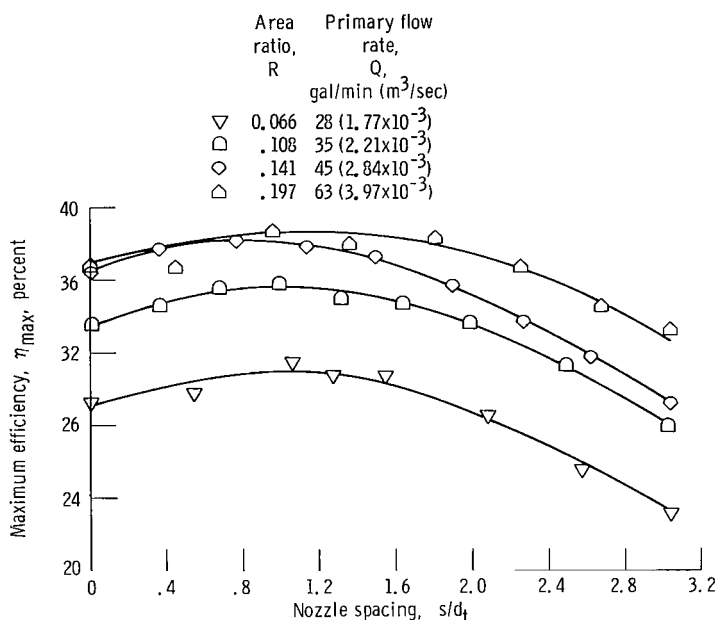


Figure 7. - Effect of nozzle spacing on maximum efficiency at four area ratio. Throat length, 3.54; diffuser angle, 2.5° .

The maximum efficiencies measured for low area ratio pumps in this investigation (31.5 to 38.7 percent) compare favorably with the best efficiencies measured for moderate to high area ratio pumps (refs. 16 to 18). They are well above values previously reported for a similar range of low area ratio pumps (refs. 12 to 15).

Comparison of theory with experiments. - The one-dimensional analysis for non-cavitating operation discussed in the Analyses section was applied to each of the configurations investigated. In previous reports the same analysis was applied to configurations having throat lengths of 7.25 diameters (ref. 3) and 5.66 diameters (ref. 5). Al-

though based on an assumption of zero nozzle spacing the theory predicted performance reasonably well for pumps of both throat lengths between nozzle spacings of 0 and 1 throat diameter. In general, there was less close agreement between experimented and predicted results for the configuration having a throat length of 5.66 throat diameters, compared to the configuration with the throat length of 7.25 diameters, but it was within the limits of acceptability. Since one of the premises of the analysis is that mixing is complete at throat exit, a greater divergence between theory and experiment would be expected as throat length is reduced.

In figure 8, theoretical and experimental values of efficiency are compared for the

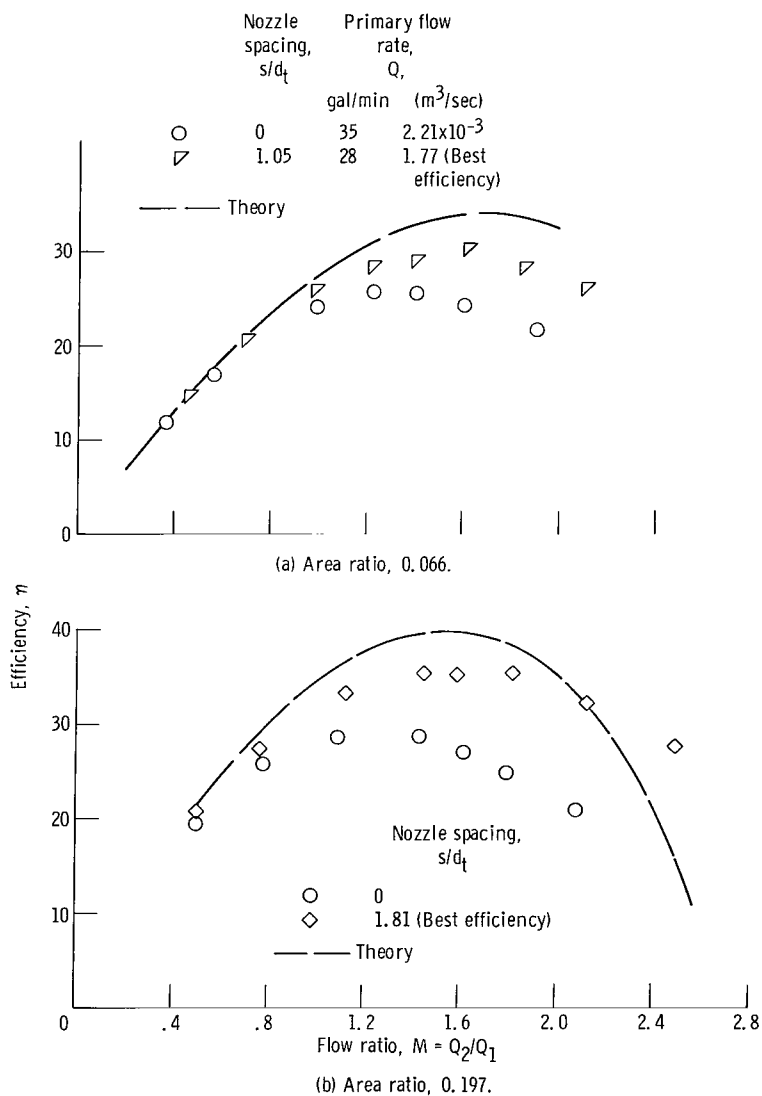


Figure 8. - Comparison of theoretical jet pump efficiency with experimental data. Throat length, 3.54; diffuser angle, 6° .

configuration having the 6° diffuser angle. Experimental data include the fully inserted and best efficiency nozzle positions at two area ratios. The agreement is poor.

The agreement is significantly better for the configurations having the 2.5° diffuser included angle (fig. 9). Since secondary inlet geometry and throat length were the same for both pump configurations (2.5° and 6° diffuser included angles), the reason for differences in performance between the two pump configurations must be attributed to the different diffuser geometries. As discussed earlier, any mixing which continues into the diffuser would have a more deleterious effect upon performance in the 6° diffuser angle pump, and this is graphically demonstrated by comparison of results shown in figures 8 and 9.

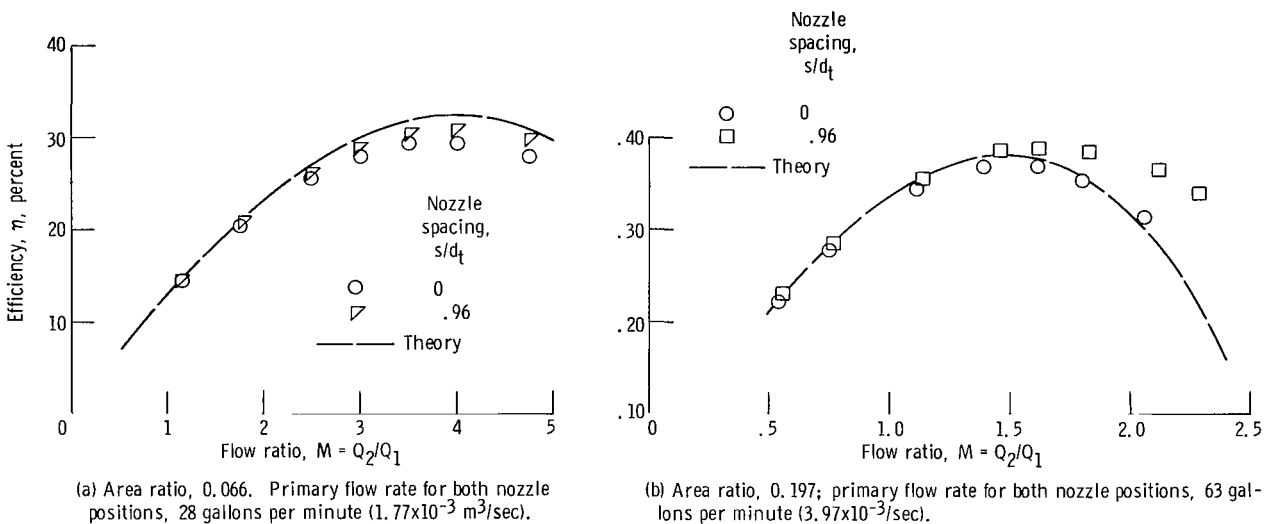


Figure 9. - Comparison of theoretical jet pump efficiency with experimental data. Throat length 3.54; diffuser angle, 2.5° .

Effect of flow ratio. - The dimensionless static pressure distributions (C_p) are plotted in figure 10 as a function of axial location. The effect of flow ratio is shown for an area ratio of 0.066 at the fully inserted nozzle position. Two effects are evident: the overall pressure level and the rate of pressure rise (i. e., pressure gradient) in the throat were reduced as flow ratio was increased. The same trends were observed at other area ratios. These effects were discussed previously in references 3 and 5.

Effect of nozzle spacing and diffuser angle. - Static pressure distributions are presented in figure 11 for a fixed flow ratio and area ratio at three nozzle positions. The nozzle positions selected were the fully inserted, the best efficiency, and a retracted position well into the low efficiency region. Two effects should be noted. First, as the nozzle was retracted the static pressure in the secondary inlet and throat increased.

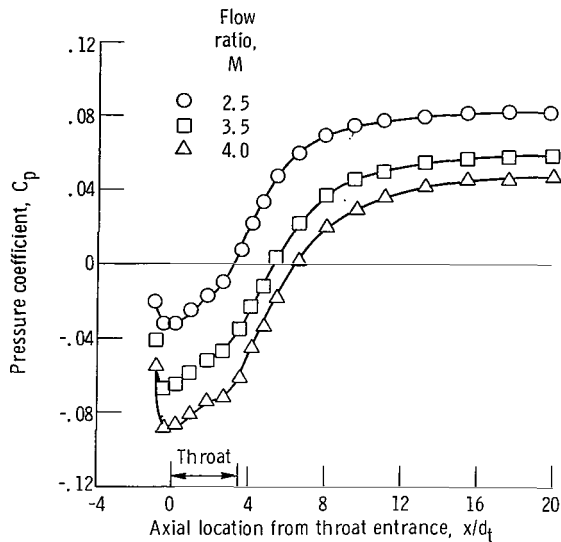


Figure 10. - Effect of flow ratio on static-pressure distributions. Throat length, 3.54; diffuser included angle, 6°; area ratio, 0.066; nozzle spacing, 0.

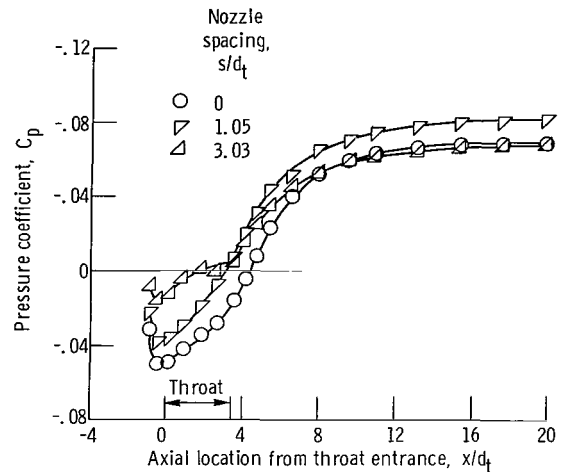


Figure 11. - Effect of nozzle spacing on static-pressure distributions. Throat length, 3.54; diffuser angle, 6°; area ratio, 0.066; flow ratio, 3.0.

This was observed and discussed previously in references 3 to 5. Second, at the largest nozzle spacings, although the positive static pressure gradient in the throat was reduced, static pressure continued to increase in the throat. This indicates that the energy losses due to friction were not great enough to counterbalance the energy addition due to mixing. Thus, even at large nozzle spacings, the greater effective mixing length was still insufficient to allow completion of mixing in the throat.

The effect of nozzle spacing on the mixing characteristics is illustrated in figure 12. Normalized total pressure distributions at three axial locations in the diffuser are shown and wall static pressure distributions are included. Data were obtained from the pump having the 2.5° diffuser included angle. Surveys of total pressure were conducted across the passage at three axial locations measured from the throat entrance, $x/d_t = 5.04$, 10.96, and 16.90. These are denoted in the figures by the letters A, B, and C, respectively. The normalized parameter \mathcal{P} was obtained by dividing the total pressure at each local radial position by the maximum total pressure (usually the midstream value) at that axial location. The normalized total pressure profile serves as an indication of the presence or absence of energy exchange at a specified axial location.

At the fully inserted nozzle position (fig. 12(a)) a significant mixing profile exists at the diffuser entrance, but has diminished before reaching a location about midway in the diffuser (B, $x/d_t = 10.9$). The small rate of change in cross-sectional area in the 2.5° diffuser permitted mixing to proceed without great energy loss. At the large nozzle spacing (fig. 12(b)) a nonuniform total pressure profile still existed in the diffuser inlet, and there was no indication of loss of static pressure in the throat due to friction. Thus,

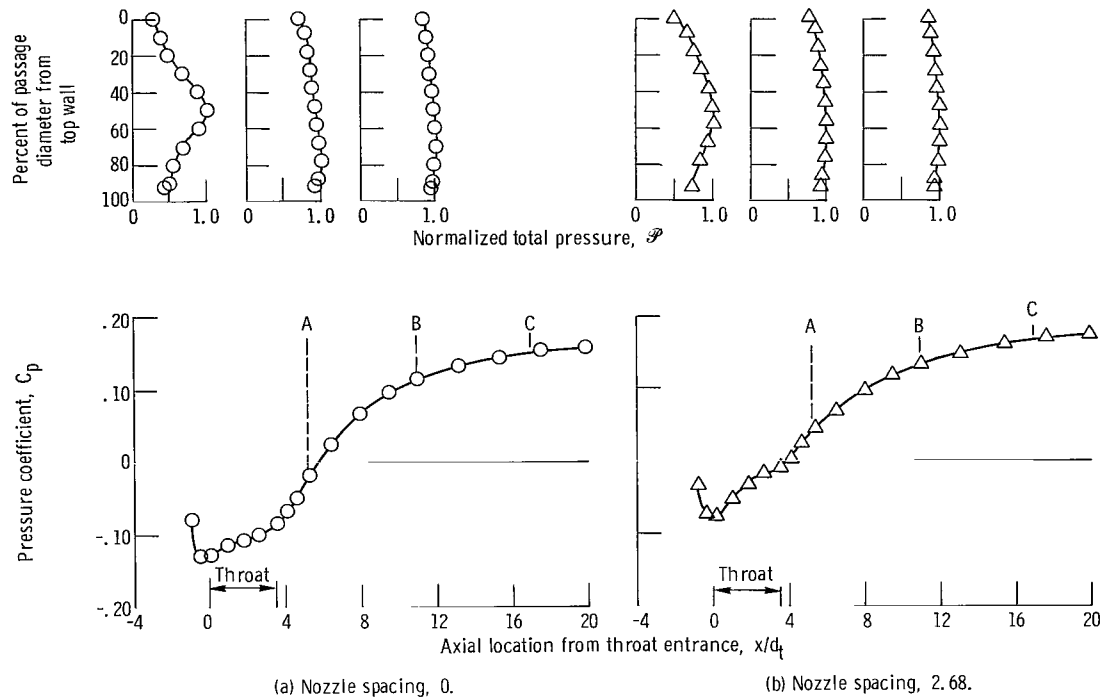
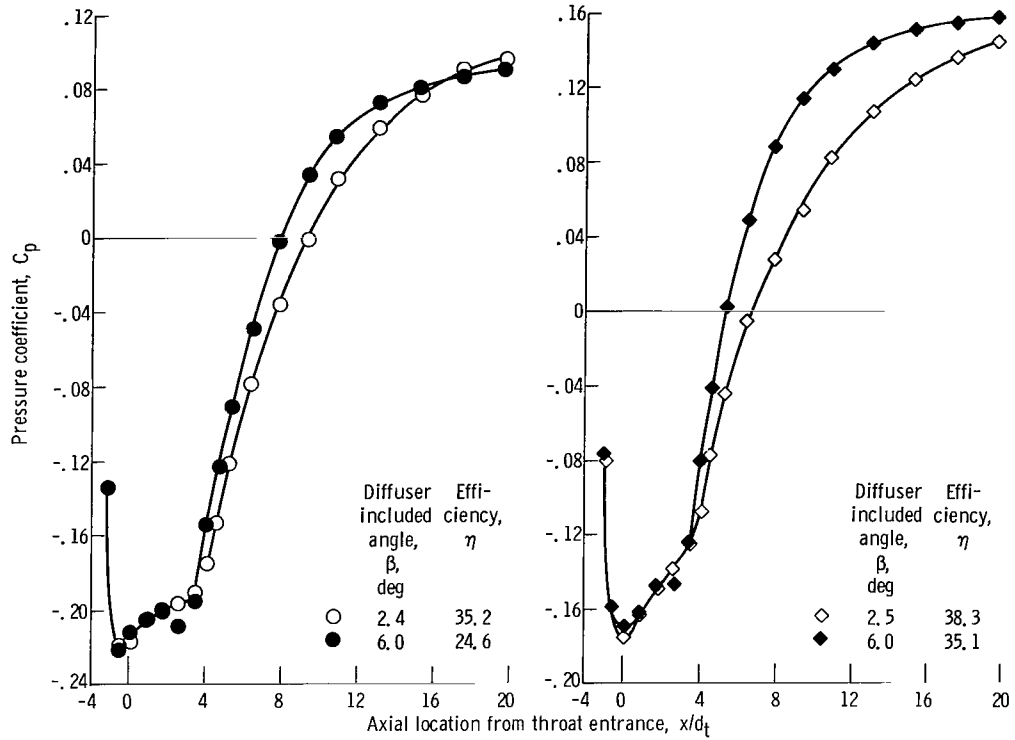


Figure 12. - Effect of nozzle spacing on total-pressure profiles. Area ratio, 0.197; flow ratio, 1.4; diffuser included angle, 2.5° .

as discussed previously, even at the large nozzle spacing, the throat did not provide sufficient length to complete mixing.

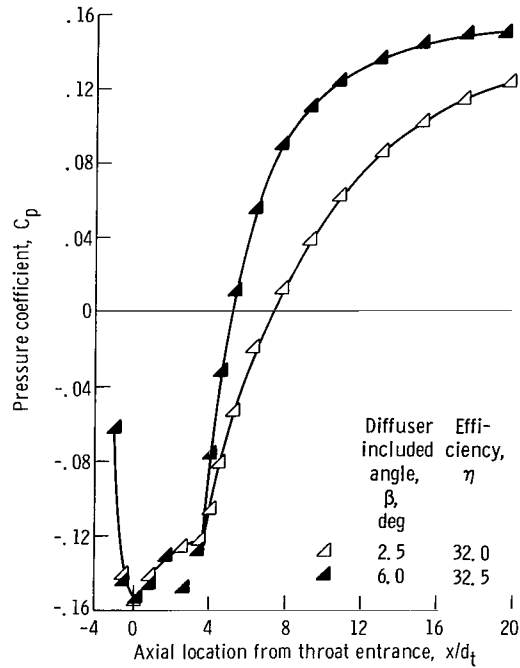
A direct comparison of the static pressure distribution in the two pumps (2.5° and 6° diffuser angles) is presented in figure 13. The static pressures are compared at three different nozzle spacings for a fixed flow ratio and area ratio. For the fully inserted nozzle position (fig. 13(a)), which provides the most nonuniform inlet velocity profile to the diffuser, the 6° diffuser did not achieve the static pressure levels achieved by the 2.5° diffuser, despite the fact that the outlet to inlet area ratio of the 6° diffuser was 7.3 as compared to 3.0 for the 2.5° diffuser. At the other two nozzle positions, which provide a greater mixing length to the fluid before entrance to the diffuser, higher static pressures were achieved in the 6° diffuser. Design diffuser performance is more likely to result if the inlet velocity profile is uniform.

It should be noted that for the nozzle spacings of $s/d_t = 0$ and 1.81 presented in figures 13(a) and (b), jet pump efficiency of the 2.5° diffuser pump exceeded that of the 6° diffuser pump, and at the large nozzle spacing of 3.03 throat diameters the efficiencies were about equal (see fig. 6). The difference between the static pressure-rise performance and the efficiency trend as nozzle spacing was varied is due to the fact that efficiency is measured in terms of total pressure (eq. (1)). Because of differences in



(a) Nozzle spacing, 0.

(b) Nozzle spacing, 1.81.



(c) Nozzle spacing, 3.03.

Figure 13. - Effect of diffuser geometry on static-pressure distributions. Throat length, $l/d_t = 3.54$; area ratio, 0.197; flow ratio, 1.8.

diffuser outlet area, improvements in jet pump static pressure-rise need not correspond to improvements in efficiency.

According to reference 10 the best conical diffuser design, from considerations of pressure rise and minimum energy loss, is one having an included angle of about 7° and a length of $12\frac{1}{2}$ to 15 times the inlet diameter. For the configurations under investigation the L/d_t of both diffusers was 16.3; thus the 6° diffuser was relatively close to the optimum for conventional diffuser design. But, as has been demonstrated, matching of a conventional diffuser with a short throat did not result in a high performance jet pump.

It is reasonable that both a high discharge static pressure and good efficiency could be obtained from a short throat jet pump if it were combined with a trumpet-shaped diffuser (fig. 14). A trumpet-shaped diffuser offers a low rate of area change in the diffuser inlet section, which in a jet pump would permit mixing to be completed more efficiently. It also has a sufficiently large outlet area to provide a high outlet static

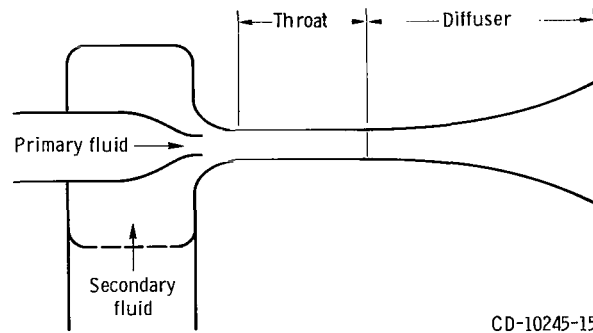


Figure 14. - Schematic representation of jet pump with trumpet-shaped diffuser.

pressure. Trumpet-shaped diffusers were investigated in reference 11 and found to provide markedly higher efficiencies than conical diffusers of the same length and outlet-to-inlet area ratio. Although unconventional in shape they may well be worth consideration for special jet pump applications.

Effect of throat length. - Maximum efficiency is plotted as a function of nozzle spacing in figure 15 for jet pumps having throat lengths of $l/d_t = 7.25$ (ref. 3), $l/d_t = 5.66$ (ref. 5), and $l/d_t = 3.54$ (this report). The diffusers of these jet pumps were not precisely alike, but were sufficiently similar to permit comparisons. Diffuser outlet areas are reasonably close to the same value; the corresponding outlet velocity heads did not differ enough to significantly alter the trends indicated. It is apparent from figure 15 that the nozzle spacing for best efficiency increased as throat length was

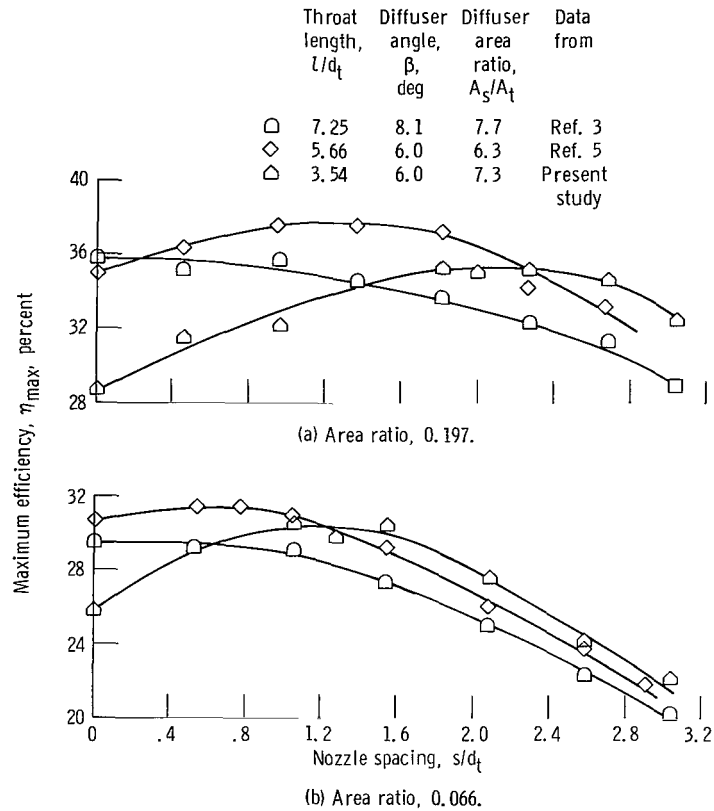


Figure 15. - Effect of throat length on most efficient nozzle position.

decreased for both area ratios considered. This emphasizes the fact that no absolute optimum nozzle spacing can be defined which is applicable to all jet pump geometrical configurations.

The effect of throat length on static pressure distributions is indicated in figure 16. At the fully inserted nozzle position ($s/d_t = 0$) no static pressure loss in the throat is indicated even in the pump having the longest throat ($l/d_t = 7.25$) and the highest jet pump static pressure rise is achieved in that pump. At largest nozzle spacings, however, the total mixing length provided by the $l/d_t = 7.25$ pump was too long and resulted in static pressure losses in the throat due to friction, and consequent penalties in jet pump outlet static pressure. At the large nozzle spacing of $s/d_t = 2.67$ the only pump which does not lose static pressure in the short throat pump ($l/d_t = 3.54$), and its overall static pressure is superior to that of the other two pumps. It is only at the large nozzle spacings, where mixing is essentially completed before the diffuser entrance, that the short throat pump exceeded the performance of the longer throat pumps.

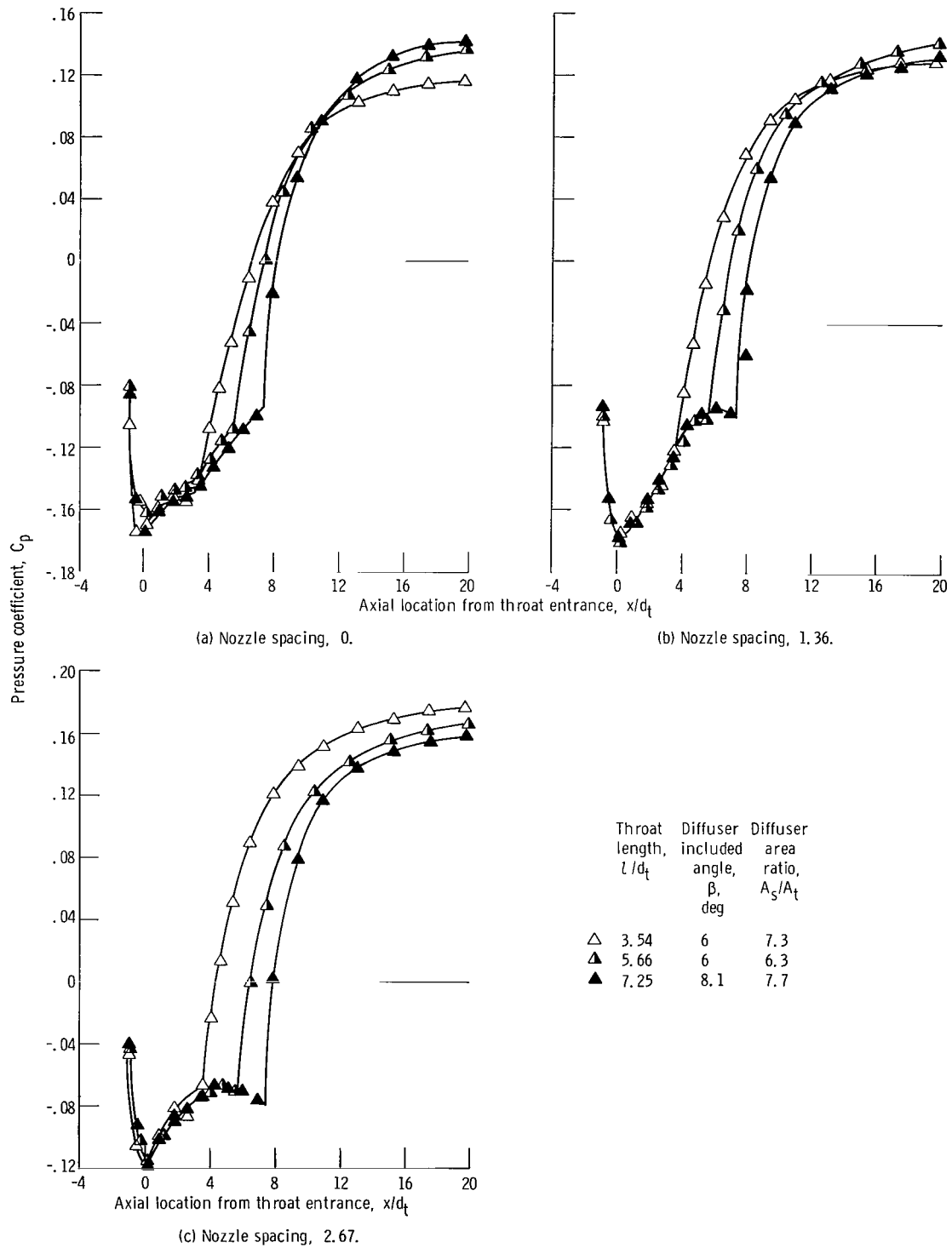


Figure 16. - Static-pressure distributions for three throat length-diffuser combinations. Area ratio, 0.197; flow ratio, 1.6.

Cavitation Performance

Experimental values of head ratio N are plotted in figure 17 as a function of net positive suction head of the secondary fluid for two of the four area ratios, $R = 0.108$ and 0.141 . For each area ratio performance is presented for three flow ratios at the fully inserted nozzle position, $s/d_t = 0$. Primary flow rate was held constant for each area ratio; therefore, the performance curves represent the effect of secondary flow rate as well as flow ratio M . The particular values of H_{SV} at which head rise deteriorates are applicable only for the flow conditions specified. As observed in previous investigations (refs. 4 and 5), the curves demonstrate a sharp, rather than a gradual, dropoff in head ratio due to cavitation. Similar curves were obtained at other nozzle spacings, other flow rates, and other area ratios.

The reasons for the trends shown by the curves are evident from figures 10 and 11. As flow ratio is increased or as nozzle spacing is reduced, static pressure in the throat decreases. Also, as absolute flow rate is increased, pressure in the throat will decrease, leading to the occurrence of cavitation at higher levels of secondary fluid net positive suction head.

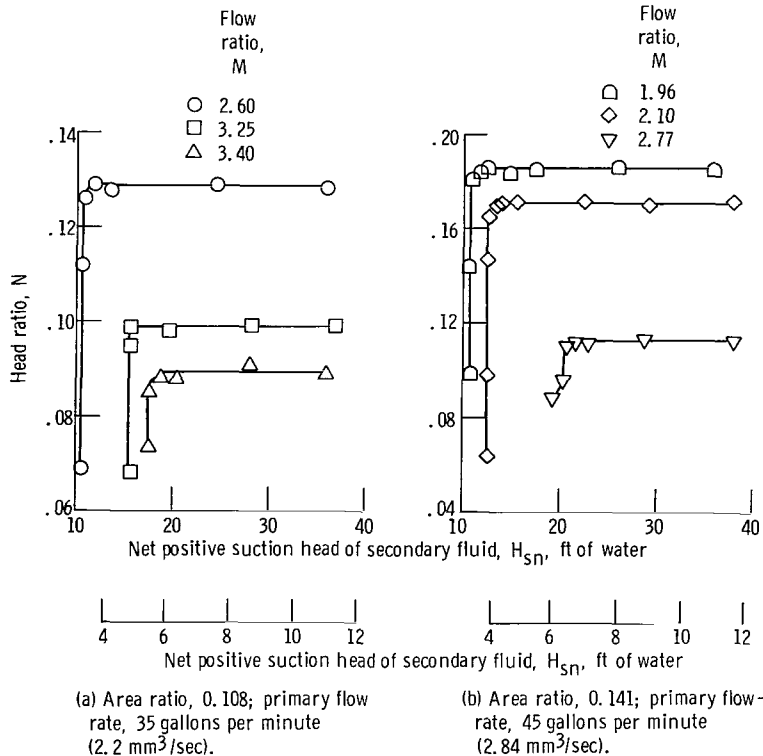


Figure 17. - Effect of inlet pressure and flow ratio on jet pump cavitation performance. Fully inserted nozzle position, 0; diffuser angle, 2.5°.

In figure 18, the values of H_{SV} at headrise dropoff are plotted as a function of flow ratio for an area ratio of $R = 0.141$. The figure demonstrates three effects: first, that for a fixed nozzle position required net positive suction head rises steeply as flow ratio is increased. The second effect indicated is the reduction in required net positive suction head as the nozzle is retracted from the throat entrance. Finally, the effect of absolute flow rate is shown. Data are plotted for two primary flow rates. For a fixed flow ratio an increase in primary flow rate produces an increase in secondary flow rate.

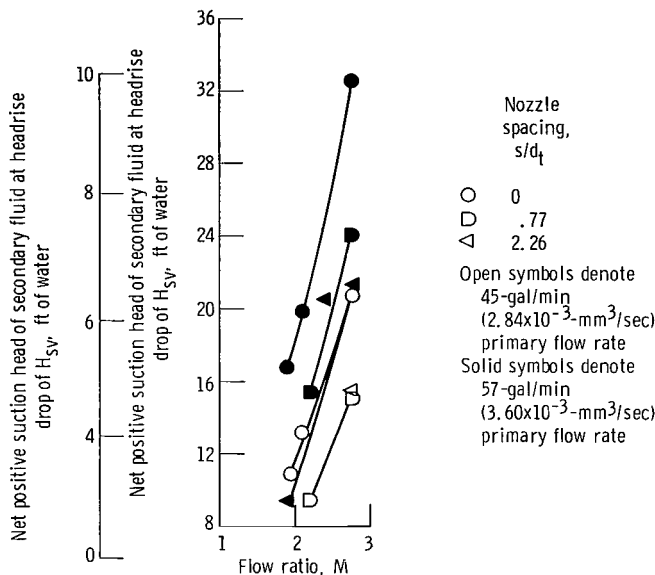


Figure 18. - Effects of flow ratio, nozzle spacing, and absolute flow rate on minimum required net positive suction head of secondary fluid. Area ratio, 0.141; diffuser included angle, 2.5°.

The higher secondary flow rate results in higher velocities through the secondary flow annulus and consequently in lower static pressures. This results in the occurrence of cavitation at higher values of H_{SV} . Thus, for a fixed flow ratio higher absolute values of flow result in loss of performance at higher values of H_{SV} . This is the third effect demonstrated by figure 18.

The cavitation prediction parameter ω (eq. (2)) is plotted in figure 19 as a function of the ratio of secondary to primary fluid velocity at throat entrance (V_3/V_N) for various values of secondary friction loss coefficient K_S (appendix B). The values of K_S of 0.09 and 0.14 are values which were measured in calibration tests for the area ratios of $R = 0.066$ and $R = 0.197$, respectively. No secondary inlet calibration tests were conducted for the $R = 0.108$ and $R = 0.141$ pumps. The data presented in figure 19 were

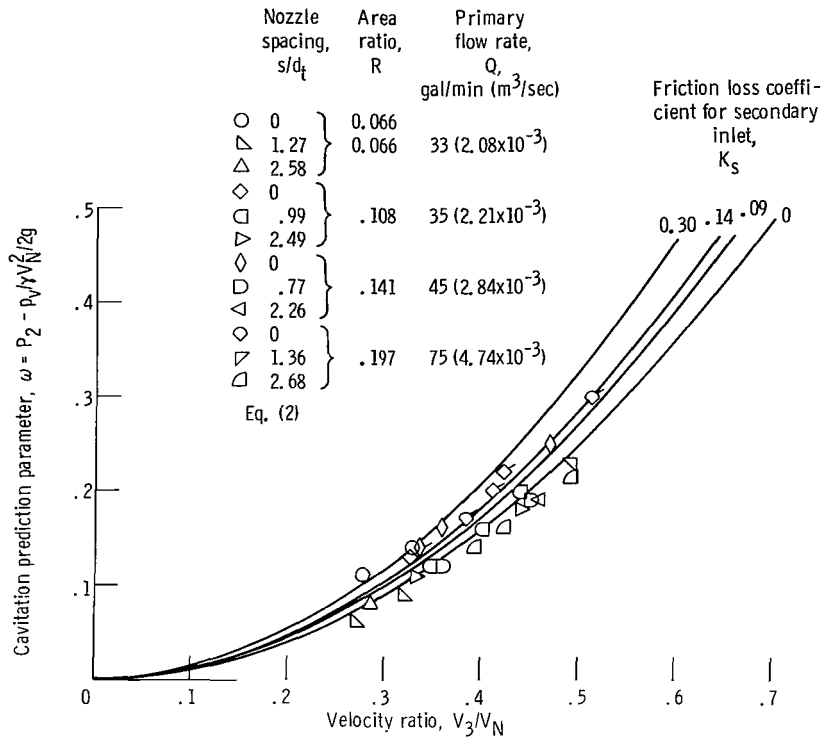


Figure 19. - Comparison of experimental jet pump cavitation results with prediction parameter (eq. (2)) for four area ratios. Throat length, U/d_t , 3.54; diffuser included angle, 2.5° .

taken at several nozzle spacings in the pump having a diffuser included angle of 2.5° . Similar results were obtained for the pumps having a diffuser included angle of 6° .

The results are quite similar to those presented in references 4 and 5. No effect of area ratio is indicated, nor does throat length appear to influence cavitation characteristics of jet pumps. As in references 4 and 5 an effect of nozzle spacing is evident. At nozzle spacings greater than about 1.0, a value of $K_s = 0$ in equation (2) may be used to predict the condition of headrise dropoff. At smaller spacings, as noted in references 4 and 5, a value of K_s appropriate to the specific inlet configuration must be used.

SUMMARY OF RESULTS

The performance of several jet pumps having the same throat diameter, the same throat length (3.54 throat diameters), and two diffuser included angles of 2.5° and 6° were evaluated in a closed-loop facility for four nozzle to throat area ratios ranging between 0.066 and 0.197. Room temperature ($80^\circ F$, $26.7^\circ C$), deaerated water was used as test fluid. Area ratio was varied by using different nozzles. Each nozzle was oper-

ated at nozzle spacings (distance nozzle exit is upstream from the throat entrance) from 0 to 3.04 throat diameters. Experimental results were compared to results from similar pumps having throat lengths of 5.66 diameters (ref. 5) and 7.25 diameters (refs. 3 and 4). Noncavitating performance data were compared to performance curves predicted by a one-dimensional analysis; cavitating performance data were compared to a prediction parameter derived from a different one-dimensional analysis.

The investigation yielded the following principal results:

1. The throat length of 3.54 throat diameters was found to be too short to allow matching with conventional diffusers (6° to 8° included angle) because of incomplete mixing at the diffuser entrance. The pump having the 2.5° included angle produced higher efficiencies than the pump having the 6° diffuser angle. Only at nozzle spacings greater than 1.0 throat diameters (longer effective mixing length) did the pump with the larger diffuser angle produce higher static pressures.

2. For the pump having the lowest area ratio investigated (0.066), a maximum efficiency of 31.5 percent was achieved in the test pump having a 2.5° diffuser included angle; the nozzle exit was positioned 1.05 throat diameters upstream from the throat entrance. For the pump having the highest area ratio investigated (0.197), a maximum measured efficiency of 38.7 percent was achieved, also in the pump having the 2.5° diffuser angle; the nozzle exit was positioned 0.96 throat diameters upstream from the throat entrance.

3. The pump having the 6° diffuser included angle (throat length of 3.54 throat diameters) generally compared unfavorably with comparable configurations having throat lengths of 5.66 and 7.25 diameters (having diffuser angles 6° and 8° , respectively). Only at large nozzle spacings where mixing is essentially completed before diffuser entrance, did the 6° pump have comparable performance to the longer throat pumps.

4. The efficiency of the pump with the 2.5° diffuser included angle (throat length of 3.54 throat diameters) compared favorably with the best efficiency previously obtained (throat length of 5.66 diam). However, because of the lower diffuser angle the pump with the 2.5° diffuser had a smaller outlet area and therefore a lower outlet static pressure.

5. The previously developed one-dimensional noncavitating analysis should be applied with discretion to jet pumps having short throats. The analysis was unable to predict performance with reasonable accuracy for the pump having the diffuser angle of 6° and throat length of 3.54 throat diameters. Because of the more gradual change in diffuser area the pump having the 2.5° diffuser provided a better correlation between theory and experiment.

6. For a fixed nozzle position, as flow ratio was increased, higher secondary inlet pressure was required to prevent cavitation. For a fixed flow ratio, as nozzle spacing from throat entrance was increased the required net positive suction head to prevent cavitation was reduced.

7. The point of performance deterioration due to cavitation was predicted with reasonable accuracy by a previously developed cavitation prediction parameter. For nozzle spacings less than 1 throat diameter an empirical loss coefficient was used. It was possible to neglect this coefficient at larger nozzle spacings.

Lewis Research Center,
National Aeronautics and Space Administration,
Cleveland, Ohio, November 27, 1968,
128-31-06-28-22.

APPENDIX A

SYMBOLS

A	area, ft ² (m ²)
C _p	pressure coefficient, $\frac{P_x - P_2}{\gamma \left(\frac{V_n^2}{2g} \right)}$
d	diameter, in. (cm)
g	local acceleration due to gravity, 32.163 ft/sec ² (9.803 m/sec ²)
g _c	dimensional constant, 32.174 (ft)(lbm)/(sec ²)(lbf) (1.0 (m)(kg)/(sec ²)(N))
H	total head of fluid, P/γ, ft (m)
H _{sv}	net positive suction head of secondary fluid, (P ₂ - p _v)/γ, ft (m)
K	friction loss coefficient
L	length, in. (cm)
l	throat length, in. (cm)
M	flow ratio, Q ₂ /Q ₁
N	head ratio, (H ₅ - H ₂)/(H ₁ - H ₅)
P	total pressure, lbf/ft ² (N/m ²)
P	normalized total pressure, P/P _{max}
p	static pressure, lbf/ft ² (N/m ²)
p _v	vapor pressure, lbf/ft ² (N/m ²)
Q	volumetric flow rate, gal/min (m ³ /sec)
R	area ratio, (A _n /A _t) = (A _n /A ₃)
s	axial spacing of primary nozzle exit from throat entrance, in. (cm)
V	velocity, ft/sec (m/sec)
x	axial distance measured from throat entrance, in. (cm)
β	diffuser included angle, deg
γ	specific weight, ρ(g/g _c), lbf/ft ³ (N/m ³)
η	efficiency, MN

ρ fluid density, lbm/ft³ (kg/m³)

ω cavitation prediction parameter, $\frac{P_2 - P_v}{\gamma \left(V_n^2 / 2g \right)}$ evaluated at total-head dropoff due to cavitation

Subscripts:

d diffuser

n primary nozzle exit plane

p primary nozzle

s secondary fluid inlet

t throat

ts test section

x linear positions measured in axial direction from throat entrance

1 primary fluid

2 secondary fluid

3 location at throat entrance

4 location at throat exit

5 location at jet pump discharge (diffuser exit)

APPENDIX B

DETERMINATION OF FRICTION LOSS COEFFICIENTS

The friction loss coefficients may be determined by flow calibration tests, as was done in the present case. Or the friction loss may be estimated, based on values in the literature (refs. 14 to 16).

Primary nozzle friction loss coefficient, K_p :

$$K_p = \frac{P_1 - p_n}{\gamma \frac{V_n^2}{2g}} - 1 \quad (B1)$$

Values of $K_p = 0.008$ and 0.036 were determined experimentally for the nozzles corresponding to area ratios of 0.066 and 0.197 , respectively. Values of $K_p = 0.017$ and 0.024 were estimated for the nozzles corresponding to area ratios of $R = 0.108$ and 0.141 , respectively. The estimate was based on an assumption of a linear change of K_p with area ratio.

Secondary friction loss coefficient K_s :

$$K_s = \frac{P_2 - p_3}{\gamma \frac{V_3^2}{2g}} - 1 \quad (B2)$$

For the fully inserted nozzle position values of $K_s = 0.09$ and 0.14 were determined for area ratios of 0.066 and 0.197 , respectively. Values of $K_s = 0.106$ and 0.120 were estimated for area ratios of $R = 0.108$ and 0.141 , respectively. The estimate was based on an assumption of a linear change of K_s with area ratio.

Throat friction loss coefficient, K_t :

$$K_t = \frac{P_3 - P_4}{\gamma \frac{V_4^2}{2g}} = f \frac{l}{d_t} \quad (B3)$$

Reynolds numbers of the flow in the throat averaged 4.4×10^5 for both test sections. For a smooth pipe this corresponds to a Darcy friction factor of $f = 0.0134$; therefore, $K_t = 0.047$.

Diffuser friction loss coefficient, K_d :

$$K_d = \frac{P_4 - P_5}{\gamma \frac{V_4^2}{2g}} \quad (\text{B4})$$

K_d is also related to the diffuser efficiency by the expression

$$K_d = (1 - \eta_d) \left[1 - \left(\frac{A_4}{A_5} \right)^2 \right] \quad (\text{B5})$$

For fully retracted nozzle positions ($s/d_t \geq 2.7$), there is generally a uniform velocity profile at inlet to the diffuser. The average diffuser efficiency determined for fully retracted nozzle positions for the 2.5° diffuser was $\eta = 88.5$ percent. This corresponds to a value of $K_d = 0.102$. The average diffuser efficiency determined for fully retracted nozzle positions for the 6° diffuser was 91.8 percent. This corresponds to a value of $K_d = 0.075$.

REFERENCES

1. Sanders, Newell D.; Barrett, Charles A.; Bernatowicz, Daniel T.; Moffitt, Thomas P.; Potter, Andrew E., Jr.; and Schwartz, Harvey J.: Power for Spacecraft. Proceedings of the NASA-University Conference on the Science and Technology of Space Exploration. Vol. 2. NASA SP-11, vol. 2, 1962, pp. 125-150.
2. Chalpin, E. S.; Pope, J. R.; and Foss, C. L.: Development of a SNAP-8 Pump for Mercury Service. AIAA Specialists Conference on Rankine Space Power Systems. Vol. I. AEC Rep. CONF-651026, vol. 1, 1965, pp. 171-185.
3. Sanger, Nelson L.: Noncavitating Performance of Two Low-Area-Ratio Water Jet Pumps Having Throat Lengths of 7.25 Diameters. NASA TN D-4445, 1968.
4. Sanger, Nelson L.: Cavitating Performance of Two Low-Area-Ratio Water Jet Pumps Having Throat Lengths of 7.25 Diameters. NASA TN D-4592, 1968.
5. Sanger, Nelson L.: Noncavitating and Cavitating Performance of Two Low-Area-Ratio Water Jet Pumps Having Throat Lengths of 5.66 Diameters. NASA TN D-4759, 1968.
6. Rouse, Hunter: Cavitation in the Mixing Zone of a Submerget Jet. LaHouille Blanche, vol. 8, Jan. -Feb. 1953, pp. 9-19.
7. Curtet, Roger: Jet Flow Between Walls. Detailed Study of Ejector Pumps. Rep. RSIC-461, Redstone Scientific Information Center, Army Missile Command, Sept. 1965. (Available from DDC as AD-473568L.)
8. Pai, Shih-i: Fluid Dynamics of Jets. D. Van Nostrand Co., Inc., 1954.
9. Waitman, B. A.; Reneau, L. R.; and Kline, S. J.: Effects of Inlet Conditions on Performance of Two-Dimensional Subsonic Diffusers. J. Basic Eng., vol. 83, no. 3, Sept. 1961, p. 349.
10. Kline, S. J.; Abbott, D. E.; and Fox, R. W.: Optimum Design of Straight-Walled Diffusers. J. Basic Eng., vol. 81, no. 3, Sept. 1959, pp. 321-331.
11. Henderson, F. D.: Effect of Profile and Length on the Efficiency of Pump Diffusers. Tech. Note 181, Rocket Propulsion Establishment, Ministry of Supply, London, Sept. 1959.
12. Lewis, R.: Jet Inducer Experimental Analysis Using Multiple Nozzles in Mercury and Water. Rep. ER-6420, TRW, Inc., May 2, 1966.
13. Lewis, R. A.: Jet Inducer Design Study for High Performance Mercury Pumps. Rep. ER-6758, TRW, Inc., Feb. 9, 1966.

14. Gosline, James E. ; and O'Brien, Morrough P. : The Water Jet Pump. Univ. California, Publ. in Eng. , vol. 3, no. 3, 1934, pp. 167-190.
15. Cunningham, Richard G. : The Jet Pump as a Lubrication Oil Scavenge Pump for Aircraft Engines. Pennsylvania Univ. (WADC TR-55-143), July 1954.
16. Mueller, N. H. G. : Water Jet Pump. Proc. ASCE, vol. 90, no. HY3, pt. 1, May 1964, pp. 83-112.
17. Vogel, R. : Theoretical and Experimental Investigation of Air Ejectors. Maschinenbautechnik, Berlin, vol. 5, 1956, pp. 619-637.
18. Hansen, Arthur G. ; and Kinnavy, Roger: The Design of Water-Jet Pumps. Part I - Experimental Determination of Optimum Design Parameters. Paper No. 65-WA/FE-31, ASME, Nov. 1965.

